Modelling the dip coating process for hot metal castings

Mark J. McGuinness* A.J. Roberts†

March 3, 2000

To appear in the proceedings of the Mathematics-in-Industry Study Group, held at Queensland University of Technology, Brisbane, Australia, 1–5 February 1999. Edited by J. Hewitt.

Contents

*School of Mathematical & Computing Sciences, Victoria University of Wellington, PO Box 600, Wellington, New Zealand; `mailto:Mark.McGuinness@vuw.ac.nz`

†Dept Maths & Comput, University of Southern Queensland, Toowoomba, Qld 4352, Australia; `mailto:aroberts@usq.edu.au`

List of Figures

1 The Problem

Toowoomba Foundry want to apply a lining to castings that provides a protective coating and is rated for potable water. They would like help with a method that involves dipping a hot casting into a fluidised bed of a thermosetting epoxy powder. The powder sticks and melts onto the hot casting, forming a film that flows then sets. The fluidised bed allows the casting to easily penetrate the powder, and gives the powder access to all surfaces of the casting.

Toowoomba produced the following list of requirements:

1. find a relationship for temperature vs time for different casting size and mass, in the oven where castings are preheated;
2. relate dipping variables (dip speed, time, flowrate of fluidising air) to film thickness;
3. understand the reasons that film thickness varies from one part of a casting to another;
4. determine the optimum hanging position to give the best access for powder to the inside and outside of castings.

Over internal surfaces of the casting we need a coating of epoxy at least $350\,\mu$m thick for transporting potable water [1]. Toowoomba Foundry would find a thickness of $400 \pm 50\,\mu$m acceptable. A casting that Toowoomba Foundry had coated by another company was available, and they also had an instrument that could be held against the casting to give the thickness of the coating at that location. We measured the thickness of epoxy coating at different locations on the casting, which was a tube with a flange at one end. We found that the coating thickness varied by about a factor of two, from $250\,\mu$m to $600\,\mu$m. The coating was typically thinnest on downward-facing surfaces and thickest on upward-facing surfaces. For more detailed results, see Figure 1. The way the casting was hung in the fluidised bed is indicated in the figure by showing the direction of gravity.

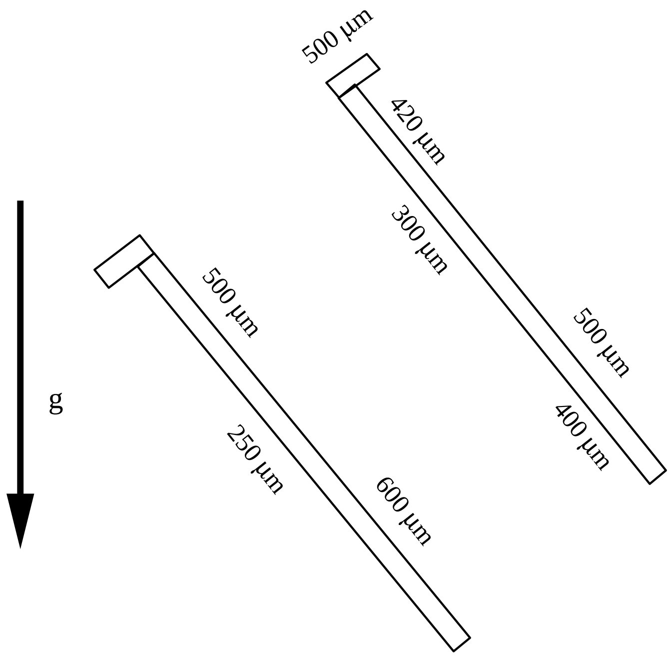

Figure 1: Schematic cross section of a commercially dip-coated cylindrical casting, showing the thicknesses of the coating as measured at various parts of the surface.

2 Fluidised Beds

Books by Davidson and Harrison [2, 3] provide good background information on fluidised beds, and a very short summary of relevant features is given here. There is also the monograph by Elmas [5], which is very relevant to this problem, since it is about dipping hot objects into fluidised polymeric powders to coat them.

Powder particles are placed on a finely perforated disk and contained laterally. Air is pumped upwards through the perforations, passing through the powder to atmosphere. When the air velocity exceeds a critical value U_{mf}, the particles become fluidised, with many of the properties of an almost inviscid fluid. Typically, for powder fluidised by air, the velocity is set somewhat higher than U_{mf}, and the excess velocity usually results in air bubbles forming and rising in the bed.

The void fraction in a fluidised bed with no bubbles is typically about $48\% \pm 4$ [13, p45], although Elmas shows it as low as 44% [5, p10]. This solid fraction is not much different from a fixed-bed loose packing of 40% or less void fraction.

When solid objects are suspended in a fluidised bed, they interfere with the vertical air flow. For surfaces facing upwards, powder slumps onto the surface. For surfaces facing downwards, powder flutters against the surface, with bubbles of air forming near stagnation points and moving away up vertical surfaces. Bubbles are observed to occur around a horizontal cylinder at a rate approximately 8 Hz from photographs [8, 13.1] of 100 μm sand particles in air blown at $1.15U_{\text{mf}}$ around a 3 cm diameter rod. In the absence of bubbles, the powder particles are practically stationary in a fluidised bed. Bubbles move and mix powder particles mainly by entrainment into their wake. Bubbles are a common occurrence in a fluidised epoxy powder such as Toowoomba are contemplating, especially near any immersed object, and we expect the effect of bubbling to be significant.

We estimate that for air to fluidise the epoxy particles, the minimum fluidisation velocity $U_{\text{mf}} \approx 4 \times 10^5\, d_e^2\, \text{m}^2/\text{s}$ where d_e is the equivalent diameter of the particles (see Eqn (2-5) in [5], or page 35 in [2]). Assuming that the epoxy particles have a mean effective diameter of 85 μm gives $U_{\text{mf}} = 2.9\,\text{mm/s}$.

An upper limit on the air velocity would be the terminal velocity of the smaller particles present, taken here to be the 53 μm diameter particles. Terminal velocity for these particles is $U_t = 121\,\text{mm/s}$.

Because of the variations in size of epoxy particles it is possible that fluidisation will result in a stratified distribution of epoxy particles — larger and heavier epoxy particles may settle to the bottom because the velocity may not be sufficient to fluidise them properly. However, there may be a Brazil nut effect — when mixed nuts are vibrated the largest move to the top. This would oppose the previous influence. Also, there is a wide range of air velocities between the minimum fluidisation velocity and the velocity at which the smaller particles are ejected from the bed, with small changes in voidage and/or bubbles accommodating the flow differences. The discussions in [9, p29,Fig. 8] and [13, pp41–2] indicate that size segregation may be negligible.

For air velocities just greater than U_{mf} the streamlines of the fluid markedly curve in towards an immersed horizontal cylinder from below [8, 13.2]. There is a smudge above the cylinder indicating that mixing of fluid has taken place. It is presumed that there is a circulation of particles at about 10 o'clock and 2 o'clock on the cylinder—upwards near the cylinder and downward away from the cylinder.

We believe that the interaction between immersed object and fluidised bed is responsible for the observed variations in coating thickness of the commercially prepared sample, and is challenging to model. For example, the work of Elmas [5] considers only vertical surfaces in fluidised beds, and ignores any bubble effects.

3 Material properties

Material properties are gathered together in this section. We consulted Dulux for epoxy properties, and one surprise last-minute value was the melting temperature of the epoxy. We conducted some tests ourselves, heating small pieces of metal with epoxy powder sprinkled on top, and noted the way the the powder initially melted, then flowed a little, filling indentations of the order of 0.1mm radius, before setting quite rapidly (in a matter of seconds).

The epoxy particles are homogeneous, with the hardener present in each piece. It is activated by high (melting) temperatures, so that melting the powder produces a flowing but viscous material, that sets in about 15 seconds.

The gel times listed below are for Scotchkote 206N epoxy, whereas Toowoomba are thinking of using NAP-GARD, for which we do not have gel times. So Toowoomba personnel conducted tests, heating iron castings to different temperatures near 200°C, and dropping a teaspoon of NAP-GARD powder onto the castings, and measured the time taken to completely solidify. Temperatures varied from 180 to 220°C, and times from 19 to 40 seconds, but there was no clearly discernible pattern, and no consistency on repeating the experiments, so no strong conclusions could be drawn on temperature dependence of setting time over this range. More details on this experiment are given later in this report.

The NAP-GARD was sieved, and the resulting percentage mass distribution is shown in Figure 2.

The thermal capacity of NAP-GARD was not available, so we used the Rilsan value of 2kJ/kg/K.

4 Time to heat castings in furnace

One task was to calculate the time required to heat typical iron castings in a forced-convection furnace. Properties of iron are to be found in the table of material properties at the end of this report. The oven will have an air speed of 6 m/s, and typical castings will have mass to area ratios of 9–12 lb/ft^2 or 45–60 kg/m^2. The actual shape of castings is variable, from simple tubes to T-bends and ninety degree bends. Some reduced air flow is to be expected

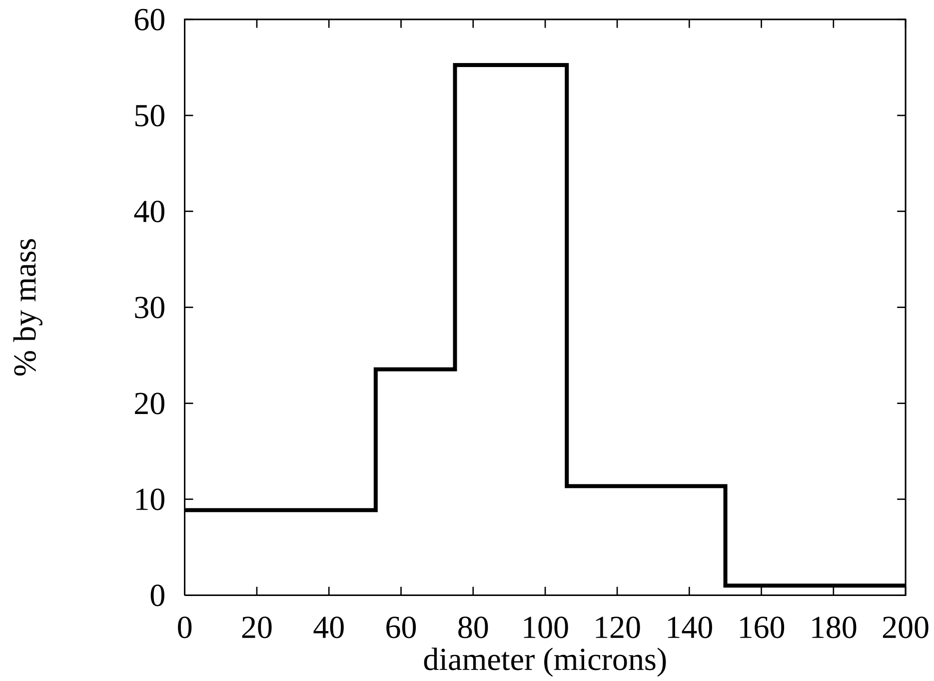

Figure 2: Percentage by weight distribution with diameter, for NAP-GARD epoxy, by sieving.

symbol	value	units	comments
k_e	0.33	W/m/°K	Epoxy thermal conductivity [4]
κ_e	1.1×10^{-7}	m^2/s	thermal diffusivity of epoxy
ρ_e	1440	kg/m^3	Epoxy density
μ_e	6–12	kg/m/s	viscosity of epoxy melt at 150 °C
σ_e	unknown	kg/s^2	surface tension coeff. of epoxy melt
T_s	60 ± 5	°C	sticking temperature of epoxy particles
T_m	70	°C	melt temperature of epoxy
	15 ± 3	s	quoted gel time at 200 °C [4]
	68 ± 10	kJ/kg	quoted energy released by epoxy setting [4]
	2.5	kJ/kg	latent heat of melting of epoxy [4]
d_e	85	μm	mean (mass weighted) particle diameter
k_r	0.29	W/m/°K	thermoplastic Rilsan properties
C_{p_r}	2.09	kJ/kg/°K	
	25	s	246C gel time of Scotchkote 206N epoxy
	30	s	232C gel time
	37	s	218C gel time
	45	s	204C gel time
ρ_c	7830	kg/m^3	metal casting density
k_c	80	W/m/°K	metal casting thermal conductivity
C_{p_c}	0.45	kJ/kg/°K	metal casting thermal capacity
	9–16	mm	thickness of castings
ρ_g	1.2	kg/m^3	air (gas) density at 20°C
ρ_g	0.7	kg/m^3	air (gas) density at 200°C
μ_g	1.8×10^{-5}	kg/m/s	viscosity of air at 20°C
μ_g	2.7×10^{-5}	kg/m/s	viscosity of air at 200°C
k_{air}	0.04	W/(m.K)	thermal conductivity of air at 500K
g	9.8	m/s^2	acceleration of gravity
h_{bed}	300	$W/(m^2\ K)$	heat transfer coeff of fluidised bed
κ_{bed}	6×10^{-7}	m^2/s	thermal diffusivity estimated for bed

Table 1: Material properties used or calculated

inside the castings, and we approximate this by reducing the surface area on the inside. So these ratios have been calculated by taking the entire outside surface area, plus half of the inside surface area of castings.

Heat flow q to the casting from the oven per unit area of casting is modelled by Newton's law,

$$q = h\Delta T\,,$$

where h is the heat transfer coefficient, and ΔT is the temperature difference between the oven and the casting.

There are several correlations giving h, and we calculated it in three different ways and obtained a range of answers that reflect the uncertainty in this parameter value.

For the correlations we need the Reynolds number, a ratio of inertial to viscous forces,

$$\mathrm{Re} = \frac{uD}{\nu}$$

where u is air velocity, D is a length (size of casting) and ν is the kinematic viscosity of air. Using $u = 6$m/s, $D = 0.2$m and $\nu = 3.8 \times 10^{-5}\mathrm{m}^2/\mathrm{s}$ at 500K, we find that Re$= 3 \times 10^4$. The value of D used here is uncertain — it is not clear how much of the air flows through (rather than around) the casting. A value of 0.2m is appropriate for flow around a typical casting that is set crosswise to the flow, but if the casting is a straight pipe presented end-on to the flow, a value of 0.02m is more appropriate (the thickness of the casting), giving Re$= 3 \times 10^3$. So the range of Reynolds numbers is Re$= 3 \times 10^3$–3×10^4.

Holman [10] has in section 6.20,

$$\mathrm{Nu} = \frac{1}{4}\,\mathrm{Re}^{0.6}\,\mathrm{Pr}^{0.38}\,,$$

where Pr is the Prandtl number, with value 0.7 for air above 350K. Nu is the Nusselt number, equal to 10.4 (if Re$= 3 \times 10^3$) or 2.6 (if Re$= 3 \times 10^4$). Nu is the ratio of convective heat flow to conductive heat flow across a slab of air of thickness L, $\mathrm{Nu} = hL/k$ where $L = 0.02$m is the thickness of the casting and $k = 0.04$W/(m.K) is the thermal conductivity of air at 500K. Then

$$h = \frac{\mathrm{Nu}\,k}{L} = 5 \text{ to } 20\,\mathrm{W}/(\mathrm{m}^2\mathrm{s})\,.$$

If on the other hand the correlation in section 6.26 of Holman (for Re in the range 100–3×10^5) is used, then

$$\mathrm{Nu} = 2 + \sqrt{0.25 + 3 \times 10^{-4}\mathrm{Re}^{1.6}}\,,$$

giving Nu in the range 12–68, and $h = 24$–$140\,\mathrm{W/(m^2s)}$.

If Table 13 in Chapter 8 of Rohsenow *et al* is used,

$$\mathrm{Nu} = D_2 \mathrm{Re}^n \ ,$$

where for Re in the range 35–5×10^3, $D_2 = 0.583$ and $n = 0.471$, and for Re in the range 5×10^3 – 5×10^4, $D_2 = 0.148$ and $n = 0.633$. Then the resulting Nusselt numbers range from 10–25, and h ranges from 20–50 $\mathrm{W/(m^2s)}$.

So there is some uncertainty in the appropriate value of h to use. In the remainder of this section we choose the value $h = 20\ \mathrm{W/(m^2s)}$, which is $h = 3.5\ \mathrm{BTU/ft^2/hr/}$. Later we check sensitivity to varying h from 10 to 50.

It is necessary to estimate whether temperature variations within the cast iron are going to be significant, requiring modelling of the conduction problem within a typical casting. The appropriate dimensionless quantity is the Biot number [14],

$$\mathrm{Bi} = \frac{hL}{k_c} \ ,$$

which is the ratio of thermal resistance within the cast iron, to thermal resistance of the surrounding air. L is the thickness of the casting, and k_c its thermal conductivity. If the Biot number is much less than one, temperature variations within the cast iron are insignificant compared to temperature differences between casting and surrounding air. In other words, temperature within the casting equilibrates much faster than the time needed to heat up the casting. We find that

$$\mathrm{Bi} = 20 \times 0.02/80 = 0.005 \ ,$$

which is indeed much less than one, so that the temperature of the casting can be regarded as essentially constant throughout its entire depth, varying only with time. This is true for the entire range of possible h values calculated above.

Then Newton's Law leads to the following formula for the temperature of the casting on the oven:

$$T - T_{\mathrm{oven}} = (T_{\mathrm{oven}} - 30)e^{\frac{thA}{WC_p}} \ ,$$

where T_{oven} is the fixed oven temperature in degrees Celsius, t is time spent in the oven, A is the casting surface area presented to the airflow in the oven, W is the mass of the casting, and C_p is the thermal capacity of cast iron. A has been determined by noting the outside area of a casting, plus half of the area inside the casting. The initial temperature of the casting has been assumed to be 30°C.

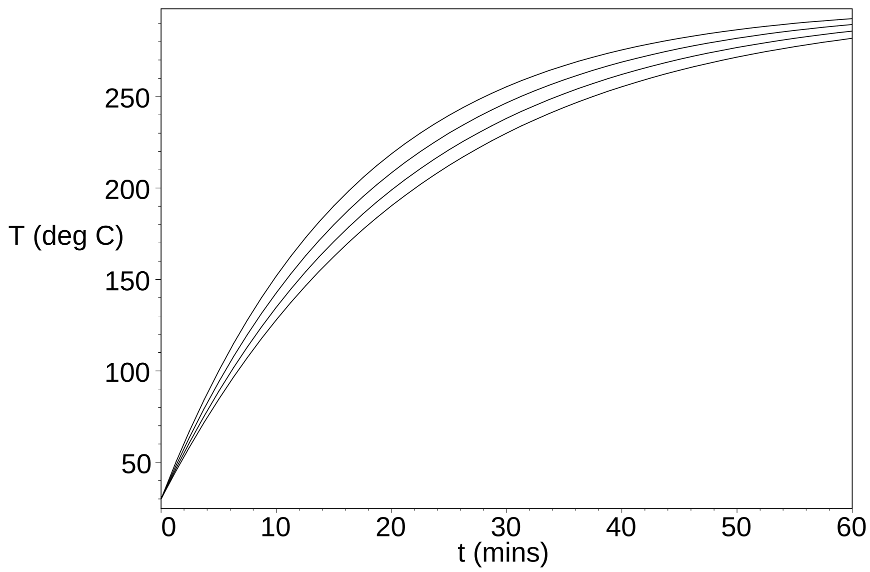

Figure 3: Temperature vs time for 300°C oven temperature with air velocity 20 ft/s, for cast iron with weight-to-area ratios 9, 10, 11 and 12 lb/ft^2, when $h = 20$.

We find that in order to heat the cast iron to (say) 200°C in about 20 minutes, an oven temperature of about 300°C is required if $h = 20$. We show plots of the temperature histories of four pieces of cast iron, with weight-to-area ratios of 9, 10, 11 and 12 lb/ft^2 (45, 50, 55, 60 kg/m^2), in Figure 3. The faster heating curves are the smaller ratios.

4.1 Sensitivity to Heat Transfer Coefficient

The value used for h, 20 W/(m^{2}s), is rather uncertain. h could be as small as 10 or as large as 50 in value. The time required to heat castings to 200°C in a 300°C oven is very sensitive to the value of h, as illustrated in Figure 4. The same weight-to-area ratios are used as in Figure 3. The lowest set of curves correspond to $h = 10$, the middle set to $h = 20$ and the highest set to $h = 50$ W/(m^{2}s). Figure 4 indicates that if h is 10, the time required to reach 200°C is 33–44 minutes, if h is 20 the time required is 16–22 minutes, and if h is 50 then the time required is 6–8 minutes. Temperature variations for different weight-to-area ratios near 200°C are about ±15°C for all cases considered.

So if different pieces of cast iron are all given the same heating time, and are heated to near 200°C, they can be expected to have actual temperatures that vary by up to ±15°C. The time required to heat pieces to

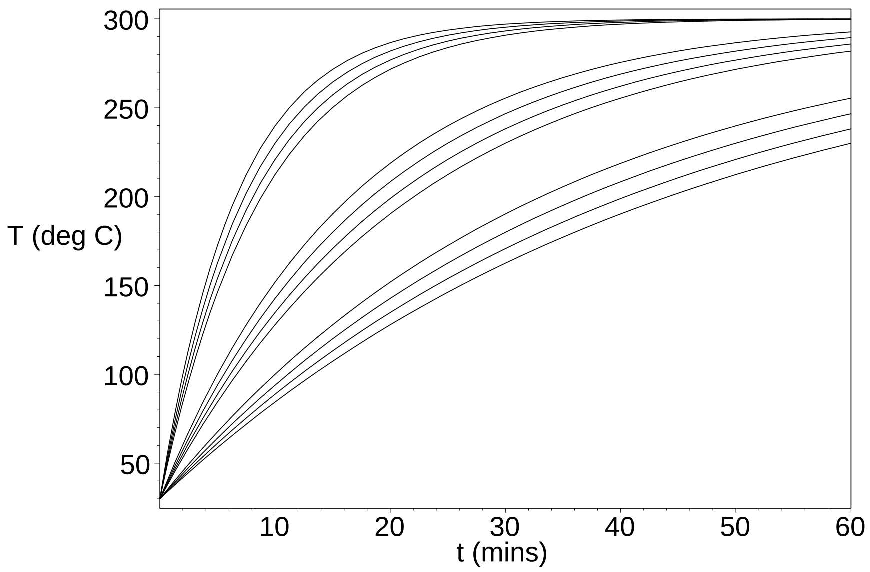

Figure 4: Temperature vs time for 300°C oven temperature with air velocity 20 ft/s, for cast iron with weight-to-area ratios 9,10,11 and 12 lb/ft^2, with $h = 10$, 20 and 50 W/(m^{2}s).

near 200°C is too sensitive to h to accurately predict, with times from 6–44 minutes, and will have to be found more accurately by experimentation with the actual oven.

5 Heat Transport in Fluidised Beds

Heat transfer between an immersed object and a fluidised bed is usually rapid. It is typically higher than that due solely to the gas flowing past, and higher than would be obtained in a fixed porous bed of particles. This is attributed to vigorous mixing of the solid phase by bubbles, which entrain the solid phase in their wake, in a model termed the *countercurrent back-mixing* model [6]. As the air velocity through a powder bed passes through the minimum fluidisation velocity U_{mf}, the effective heat transfer coefficient rises rapidly as illustrated in Figure 5. For small light particles such as the epoxy we are dealing with, the velocity U_{opt} of maximum heat transfer is close to the terminal velocity of the particles.

We do not think that the fluidised bed will heat up significantly by having the hot castings bathed in it—the continuous air flow and high degree of mixing should be enough to maintain reasonably constant bed temperature [5, p9]. We note that the gas will be quite cool since it comes from a

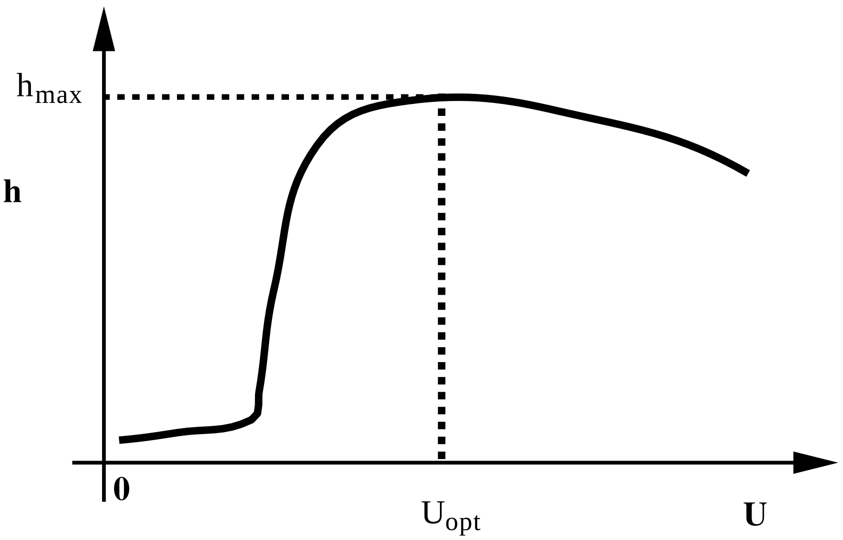

Figure 5: Effective heat transfer between an immersed object and a typical fluidised bed, versus fluid velocity in the bed.

compressed tank.

5.1 Heat Transfer Coefficient

An empirical correlation ([6], p515) for heat transfer to a heavy spherical probe in an air-fluidised bed uses the Archimedes number,

$$\mathrm{Ar} \equiv \frac{g d_e^3}{\nu^2} \left(\frac{\rho_e - \rho_g}{\rho_g} \right) \ ,$$

where g is the gravitational acceleration, d_e is the diameter of a sphere with equivalent surface area to the particles in the fluidised bed, ν is the kinematic viscosity of air, ρ_e is the density of the epoxy particles being fluidised, and ρ_g is the density of air. Using values appropriate to a temperature of 500K gives Ar= 8.35. For Ar in the range 30 to 2×10^5, the correlation

$$\mathrm{Nu}_{\mathrm{max}} \equiv h_{\mathrm{max}} d_e / k_{\mathrm{air}} = 0.86\,\mathrm{Ar}^{0.2}$$

is appropriate. The Nusselt number in this case is the ratio of heat flow to the fluidised bed to the heat that would be conducted across a slab of air of thickness equal to one particle diameter.

This gives $\mathrm{Nu}_{\mathrm{max}} = 1.3$. The resulting value for the maximum heat transfer coefficient from an immersed object to our fluidised bed is $h_{\mathrm{max}} =$ 600 W/(m^{2}K). Note that for small light particles this maximum will only be realised at high air velocities, near ejection rates. However, since the correlation was obtained under actual experimental conditions, it will include the effects of bubbles. The actual heat transfer coefficient will be less than this, and we will take the value $h_{\text{bed}} = 300\ \text{W}/(\text{m}^2\text{K})$ for estimation purposes in the following. This is a highly uncertain estimate for the value of this parameter, and could be out by several orders of magnitude.

Then the Biot number for a hot casting immersed in our fluidised bed is

$$\text{Bi} = \frac{h_{\text{bed}} L}{k_c} = \frac{300 \times 0.02}{80} = 0.075 \ ,$$

which is much less than one, so that temperature variations spatially within the casting are negligible on the time scales associated with heat loss to the fluidised bed — the temperature in the cast iron drops but is almost the same everywhere in the casting.

5.2 Change in temperature of castings

We estimate the change of casting temperature during the time it is immersed in the fluidised bed, by using the standard heat balance (eg, Elmas [5] p. 32) for the heat lost in time Δt from a piece of cast iron of volume V and surface area A which changes temperature T by an amount ΔT:

$$\Delta T V \rho_c C_{pc} = -A h_{\text{bed}} (T - T_{\text{bed}}) \Delta t \ .$$

Sending Δt to zero leads to the differential equation

$$\frac{dT}{dt} = -\frac{A h_{\text{bed}}}{V \rho_c C_{pc}} (T - T_{\text{bed}}) \ ,$$

with solution

$$T = T_{\text{bed}} + (T_0 - T_{\text{bed}}) \exp\left(\frac{-A h_{\text{bed}}}{V \rho_c C_{pc}} t \right) \ ,$$

where T_0 is the initial casting temperature. The decrease in casting temperature is then

$$\Delta T = (T_0 - T_{\text{bed}}) \left[1 - \exp\left(-\frac{A h_{\text{bed}}}{V \rho_c C_{pc}} t \right) \right] \ .$$

A plot of the decrease in temperature, using $T_0 - T_{\text{bed}} = 200°\text{C}$, $h_{\text{bed}} = 300\ \text{W}/\text{m}^2/\text{K}$ and using the four typical weight-to-area ratios (WoA $\equiv V\rho_c/A$) 45, 50, 55 and 60 kg/m^2 appears in Figure 6. Note that for the first ten seconds the solution is nearly linear, and the change in temperature is adequately described by

$$\Delta T = (T_0 - T_{\rm bed}) \left(\frac{A h_{\rm bed}}{V \rho_c C_{pc}} \right) t \approx 133t/{\rm WoA} \ .$$

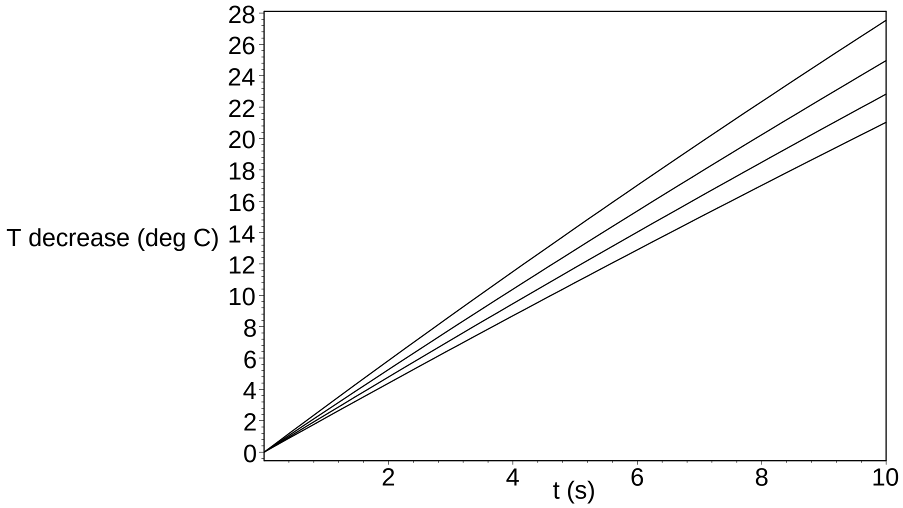

Figure 6: The temperature changes estimated for the cooling of castings in a fluidised bed of epoxy. The four curves are for weight-to-area ratios of 45, 50, 55 and 60 kg/m^2, with the faster cooling rates applying to the smaller ratios.

The temperature changes to be expected in the iron castings after five seconds of immersion in the fluidised bed, then, are about 10–15°C, small compared with the expected initial temperature of 200°C.

5.3 Heat transport modelled by rotation of fluidised particles

A new model of thermal transport through a fluidised bed is presented here, and is based upon particles which rotate in place due to unbalanced stresses from the airflow past them. Assume that particles of diameter d rotate in a time τ in a mean thermal gradient T'. The rotation could be due to being in a shear flow in which case $\tau = 2\pi/u'$, or it could be due to unbalanced shear forces from the interstitial forces. The rotation advects heat.

Heat transport is assumed in this model to be determined by the transfer from one particle to the next. Consider the schematic situation shown in Figure 7. Suppose any one part of a particle is in contact with its neighbour for a fraction α of a period τ. In that time the temperature

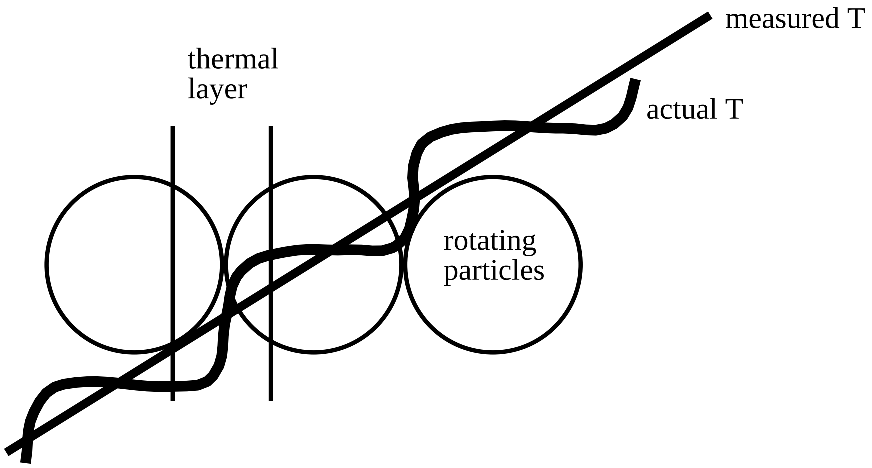

Figure 7: A conceptual illustration of a string of rotating particles, which carries heat in a mean temperature field by rapid diffusion across narrow boundary layers between particles.

difference penetrates a distance $\sqrt{\alpha\kappa_e\tau}$ into the particle. Hence the flux of heat from one particle to the other is proportional to the fraction of contact area, $\sin(\pi\alpha)$, the particle diffusivity, κ_e, and the actual temperature gradient in the interparticle layer, $T'_{\text{actual}} = T'd/(2\sqrt{\alpha\kappa_e\tau})$. We write

$$\frac{dT}{dt} = \sin(\pi\alpha)\,\kappa_e\,T'_{\text{actual}} = \kappa_{\text{eff}}T' \ .$$

For small contact α the effective thermal diffusivity is then

$$\kappa_{\text{eff}} \approx \frac{\pi\sqrt{\alpha}}{2}\sqrt{\frac{\kappa_e d^2}{\tau}}\,, \tag{1}$$

where we do not believe any significance holds for the constant in front of the square root sign, except that α could be fairly small. Arguments about the heat carried across the particle by the rotation give a similar flux and hence a similar effective diffusivity. This effective diffusivity could be viewed as the geometric mean of the particle diffusivity and and a diffusivity due to particle rotation, d^2/τ. This effective diffusivity could be considerably larger than κ_e. In particular note that, other things being constant, it is proportional to the particle diameter. Also, if we assume that in a fluidised bed the shear forces are proportional to $U - U_{\text{mf}}$ then $\tau \propto 1/(U - U_{\text{mf}})$ and hence $\kappa_{\text{eff}} \propto \sqrt{U - U_{\text{mf}}}$ which could explain the steep rise in thermal diffusivity seen upon fluidisation [6].

5.4 Estimated Thermal Diffusivity of Bed

Davidson and Harrison [2], p. 488, give an empirical formula for the ratio of effective thermal conductivity of a fluidised bed to the thermal conductivity of the fluidising air k_{air} ,

$$\frac{k_{\text{bed}}}{k_{\text{air}}} \approx 1 + \frac{(1-\epsilon)\left(1 - \frac{k_{\text{air}}}{k_e}\right)}{\frac{k_{\text{air}}}{k_e} + 0.28\epsilon^{0.63}\left(\frac{k_e}{k_{\text{air}}}\right)} , \tag{2}$$

where ϵ is the void fraction of the bed, here taken to be 0.48, and k_e is the epoxy thermal conductivity. Using $k_{\text{air}} = 0.03$ W/(mK) (at 400K), this gives

$$k_{\text{bed}} \approx 0.1 \text{ W/(mK)} . \tag{3}$$

Note that this empirical result includes the effect of bubbling, and may not be entirely appropriate for an upwards-facing surface with particles slumped onto it. Nevertheless, we intend to use this result for upwards-facing surfaces later.

Elmas [5] estimates the effective thermal capacity of the fluidised bed by using packed-bed theory, and has

$$\langle \rho C_p \rangle_{\text{bed}} \approx (1-\epsilon)\rho_e C_{pe} + \epsilon \rho_g C_{P_g} \approx 1.6 \times 10^6 \text{ W/(m}^3\text{K)} , \tag{4}$$

giving an effective thermal diffusivity for the fluidised bed as

$$\kappa_{\text{bed}} = \frac{k_{\text{bed}}}{\langle \rho C_p \rangle_{\text{bed}}} \approx 6 \times 10^{-7} \text{ m}^2\text{/s} . \tag{5}$$

This is a highly uncertain parameter, and could be out by several orders of magnitude.

6 Modelling Coating Growth

Three models have been proposed to predict the growth of coating thickness for a hot casting immersed in a fluidised bed of epoxy particles. The first is appropriate for surfaces facing upwards, with powder slumped onto the surface due to blocking of upwards airflow, and is a simple conduction model. Elmas [5] also finds such a model to be useful for vertical surfaces. The coating thickness is determined by the penetration depth of the melting temperature.

The second model (a melted-on model) is designed for downwards facing surfaces, with powder intermittently present at the surface, due to significant bubbling effects. This model has a coated region where the epoxy has stuck onto the iron, and simple heat transfer from the coating to the fluidised bed.

The third model is a modification of the melted-on model, in which we assume a linear temperature profile in the melted coating region in order to obtain analytic results.

Surface temperature is the factor that determines whether a particle of epoxy will stick to the casting or not. Our models all assume that the casting temperature is constant in space and in time, consistent with the above estimates.

6.1 Simple Conduction Model

The coating thickness is obtained by solving a pure conduction problem in the fluidised bed, and ignoring any changes consequent upon particles sticking to the casting. The iron casting is assumed to have constant temperature, higher than the temperature at which the epoxy sticks. Temperature in the fluidised bed is assumed to obey a one-dimensional conduction model with uniform thermal properties throughout the coating and the bed.

The coating properties are taken to be the same as the bed properties. This is despite the fact that most of the coating will be melted, suggesting a more complicated two-layer model might be more appropriate.

The coating then extends into the bed a distance determined by the temperature at which particles stick, as illustrated in Figure 8. This model is expected to be more appropriate for upwards-facing surfaces, with powder slumped onto the surface. The same model was used by Elmas [5] for vertical surfaces, but there were no bubbles in his experiments, since the immersed objects were thin vertical sheets.

We set up a nondimensionalised conduction problem modelling heat transport into the fluidised bed in the usual way, to obtain

$$\frac{\partial T}{\partial t} = \frac{\partial^2 T}{\partial x^2} \ , \tag{6}$$

where

$$T \equiv \frac{T_{\text{bed}} - T_i}{T_{\text{iron}} - T_i} \ , \tag{7}$$

and where $T_{\text{bed}}(x, \tilde{t})$ is the temperature in the fluidised bed at time $\tilde{t}$ seconds and a distance x metres away from the casting surface, T_i is the initial bed temperature, T_{iron} is the temperature of the iron casting (assumed constant),

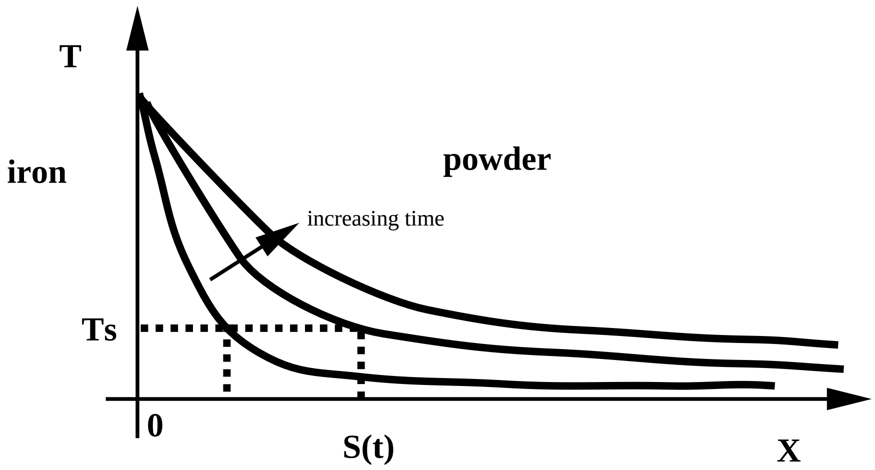

Figure 8: A sketch illustrating temperature changes in fluidised bed and resulting coating thickness for the simple conduction model.

and time has been rescaled as

$$t = \kappa_{\text{bed}} \tilde{t} \ , \tag{8}$$

and κ_{bed} is the effective thermal diffusivity of the fluidised bed. The distance x could be rescaled, for example on the casting thickness, but there is no natural length-scale in this semi-infinite problem.

Then initial and boundary conditions are $T = 1$ at $x = 0, \forall t$, and $T = 0$ at $t = 0, \forall x \neq 0$. The surface of the iron is set at $x = 0$, and time origin is the instant of immersion of the cast iron. The solution is then

$$T = \operatorname{erfc}\left(\frac{x}{2\sqrt{t}}\right) \ , \tag{9}$$

where the complementary error function is defined as

$$\operatorname{erfc}(z) \equiv \frac{2}{\sqrt{\pi}} \int_z^\infty e^{-y^2}\, dy \ = 1 - \operatorname{erf}(z) \ , \tag{10}$$

and where the error function is $\operatorname{erf}(z) \equiv \frac{2}{\sqrt{\pi}} \int_0^z \exp(-y^2)\, dy$.

The coating thickness is the penetration depth $s(t)$ of the temperature at which particles stick. s is written

$$s = 2\beta\sqrt{t} \ , \tag{11}$$

where β is given implicitly by

$$T_s = \operatorname{erfc}(\beta) \ . \tag{12}$$

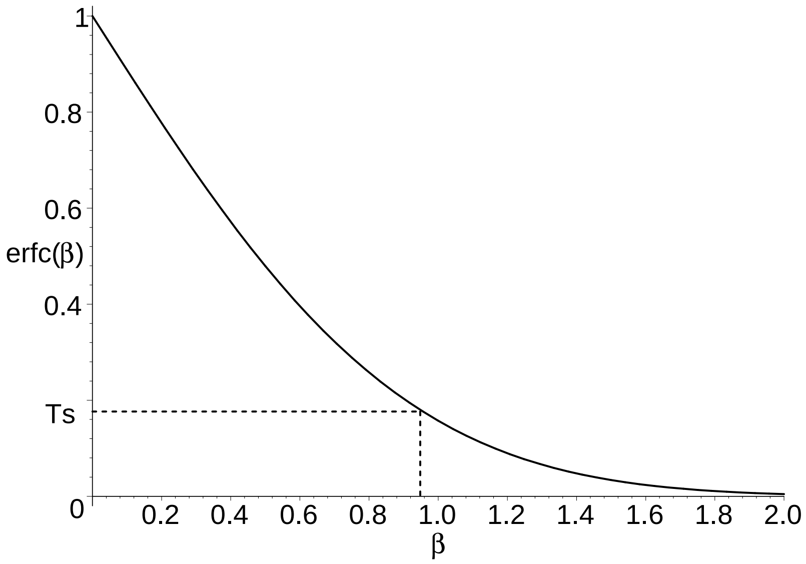

Figure 9: A plot of erfc(β), illustrating the determination of β given T_s.

T_s is the nondimensional temperature at which particles stick to the coating surface,

$$T_s \equiv \frac{T_{\text{stick}} - T_i}{T_{\text{iron}} - T_i} ,$$

where T_{stick} is 60°C for NAP-GARD.

The growth rate of the coating is proportional to β. Figure 9 shows erfc(β), which decays to zero as β increases, and shows how β depends on the value of T_s. As T_s is reduced, clearly β increases.

6.2 Melted-on Model

In this model, expected to be more suitable for downward-facing surfaces, and for vertical surfaces in the presence of bubbles, the thermal conduction problem is solved within the stuck-on coating layer, and a simple Newton's law is used for heat loss to the fluidised bed from the layer. See Figure 10 for an illustration. The temperature at the surface of the coating is assumed to be the controlling factor in determining surface growth.

When there is bubbling (or periodic slumping of powder away from the surface and then hitting it again), we assume that there is still plenty of powder delivered to the immersed surface, so that if the temperature at

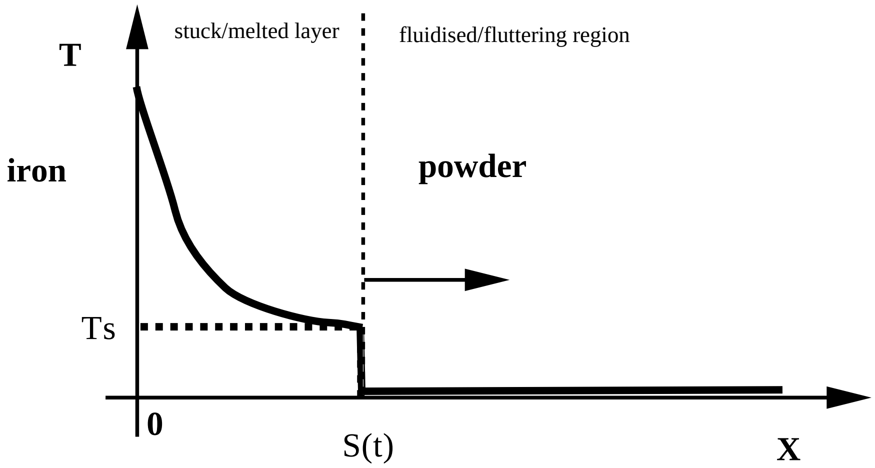

Figure 10: A sketch illustrating the melted-on model.

the coating surface is at or above the sticking temperature, a particle will stick to it immediately. However, we expect that the fluttering and mixing consequent upon the bubbling will be consistent with an almost constant temperature in the fluidised bed next to the coating, with heat loss to the bed dependent on an effective heat transfer coefficient.

Note that this model is a simplification of that of Leong *et al* [11], which has the additional freedom that the temperature of the iron casting is allowed to change. Our calculations suggest that this is not an important factor.

We make the same nondimensionalisations as for the Simple Conduction Model above. Note that T_i is now the unchanging temperature of the fluidised bed. The only temperature changes are in the coating, which has the same temperature as the iron casting at $x = 0$, and has a temperature equal to the powder sticking temperature at its outer surface, where temperature jumps from T_{stick} to T_i.

We have heat conduction within the coated layer, constant temperature in the iron, and growth of the layer thickness according to conservation of energy at the coating surface. The appropriate thermal diffusivity to use here is clearly that of the melted epoxy, not that of the fluidised bed. Hence the time scale in the melted-on model will not be the same as the time-scale of the simple conduction model. Bed properties are simplified to appear only as a heat transfer coefficient between the coating and the bed.

The model equations are then

$$\frac{\partial T}{\partial t} = \frac{\partial^2 T}{\partial x^2} \tag{13}$$

with initial and boundary conditions $T = 1$ at $x = 0$, $\forall t$ (iron surface), $T = 0$ when $t = 0$, $\forall x \neq 0$, and $T = T_s$ at $x = \mathcal{S}(t)$ (where the coating meets the bed). Conservation of energy at the coating surface gives

$$T_s \frac{d\mathcal{S}}{dt} = -\frac{\partial T}{\partial x} - h(T_s) \; , \tag{14}$$

where $h(T_s)$ usually takes the form HT_s, where $H = h_{\text{bed}}/k_e$, and h_{bed} is the effective heat transfer coefficient between coating and bed, and k_e is the thermal conductivity of the melted-on epoxy.

That is, the surface moves at a velocity that depends on the heat conducted to it from the iron through the coating, and on the heat that is conducted away from the surface to the fluidised bed. Note that the full form of h is given by

$$h(T_s) = \frac{h_{\text{bed}}}{k_e} \left(\frac{T_{\text{stick}} - T_i}{T_{\text{iron}} - T_i} \right) \; .$$

6.2.1 Zero heat transfer to bed

An analytic solution is possible when there is zero heat transfer to the bed, $h(T_s) = 0$, and is useful for understanding the more general case when $h(T_s) \neq 0$. If $h(T_s) = 0$, the solution is

$$T = 1 - A\,\text{erf}(x/(2\sqrt{t}\,)) \; , \tag{15}$$

where A is a constant, determined below. We define $\mathcal{S} = 2\alpha\sqrt{t}\,$, and note that at $x = \mathcal{S}(t)$

$$T_s = 1 - A\,\text{erf}(\alpha) \, , \tag{16}$$

The boundary condition (14) at $x = \mathcal{S}(t)$ gives A,

$$\alpha T_s = \frac{A}{\sqrt{\pi}} e^{-\alpha^2} \; . \tag{17}$$

Solving equations (16) and (17) simultaneously gives

$$T_s = 1 - \sqrt{\pi}\, T_s \alpha\, e^{\alpha^2} \text{erf}(\alpha) \; , \tag{18}$$

which implicitly defines α and hence the coating thickness $\mathcal{S}$.

Setting $h(T_s)$ to zero is a good approximation for early times, such that

$$T_s \frac{d\mathcal{S}}{dt} \gg h(T_s) \; ,$$

that is,

$$T_s \frac{\alpha}{\sqrt{t}} \gg h(T_s) \; ,$$

which gives

$$t \ll \left(\frac{T_s\alpha}{h(T_s)}\right)^2 \,,$$

or

$$t \ll \left(\frac{\alpha k_e}{h_{\text{bed}}}\right)^2 \,. \tag{19}$$

Using $k_e = 0.33$, $\alpha \approx 1$ and $h_{\text{bed}} \approx 300$ gives

$$t \ll 10^{-6} \,,$$

that is, using $\kappa_e \approx 10^{-7}$,

$$\tilde{t} \ll 10 \text{ s} \,.$$

That is, dipping time needs to be much less than ten seconds if the early time approximation of zero heat transfer is to be valid.

So if castings are dipped for 5 seconds, the early time approximation of setting $h(T_s)$ to zero for the melted-on model is beginning to become a little inaccurate, but will still give reasonable estimates (slight over-estimates) of coating growth.

6.2.2 Nonzero heat transfer to bed

Coating thickness grows without limit in the above case of zero heat flux to the fluidised bed. In the case of nonzero heat flux to the fluidised bed, an analytic solution is not available. However, the early time behaviour of the coating thickness is the same as in the zero heat flux case, and the late time behaviour of the thickness is to asymptote to the value determined by the balance

$$\frac{\partial T}{\partial x} = -h(T_s) \,. \tag{20}$$

The sketch in Figure 11 illustrates typical behaviours of coating thickness versus time for the simple conduction model and the melted-on model with zero and nonzero heat transfer to the bed.

6.3 Linear Temperature Model

If we assume a linear temperature profile in the melted-on coating, an approximate analytic solution results. That is, we take

$$T = 1 - \frac{x(1 - T_s)}{\mathcal{S}(t)} \,. \tag{21}$$

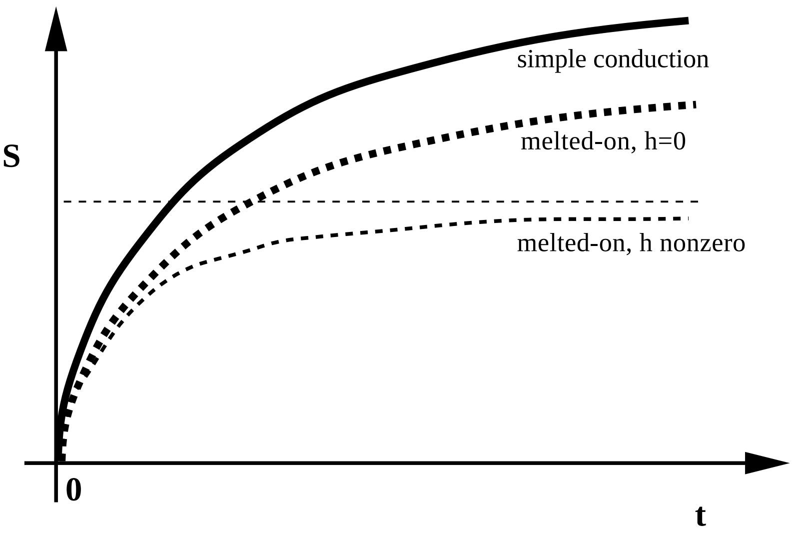

Figure 11: A sketch illustrating the qualitative behaviours of coating thickness S versus time for the simple conduction model and for the melted-on model with zero and non-zero heat transfer to the bed.

Then equation (14) becomes

$$\frac{d\mathcal{S}}{dt} = \frac{1}{T_s'\mathcal{S}} - H \,, \tag{22}$$

where $T_s' \equiv T_s/(1-T_s)$, and recall that $H = h_{\text{bed}}/k_e$. This separates and integrates to give the analytic solution

$$\mathcal{S}' + \ln\left(1-\mathcal{S}'\right) = -tH^2T_s' \,, \tag{23}$$

which defines $\mathcal{S}'$ implicitly, where

$$\mathcal{S}' \equiv H\mathcal{S}T_s' \,.$$

The value of $\mathcal{S}'$ defined by equation (23) is plotted against $t\,H^2T_s'$ in Figure 12. Note the horizontal asymptote at $\mathcal{S}' = 1$, that is, when $\mathcal{S} = 1/(T_s'H) = (1-T_s)/(HT_s)$. This is the maximum possible value for coating thickness, reached when the heat conducted to the coating surface from the iron through the coating matches the heat lost from the coating surface to the fluidised bed. As also derived by Gutfinger and Chen [7], this limiting coating thickness for downwards-facing surfaces is in dimensional terms equal to

$$\frac{k_e}{h_e}\left(\frac{T_{\text{iron}} - T_{\text{stick}}}{T_{\text{stick}} - T_i}\right) \,.$$

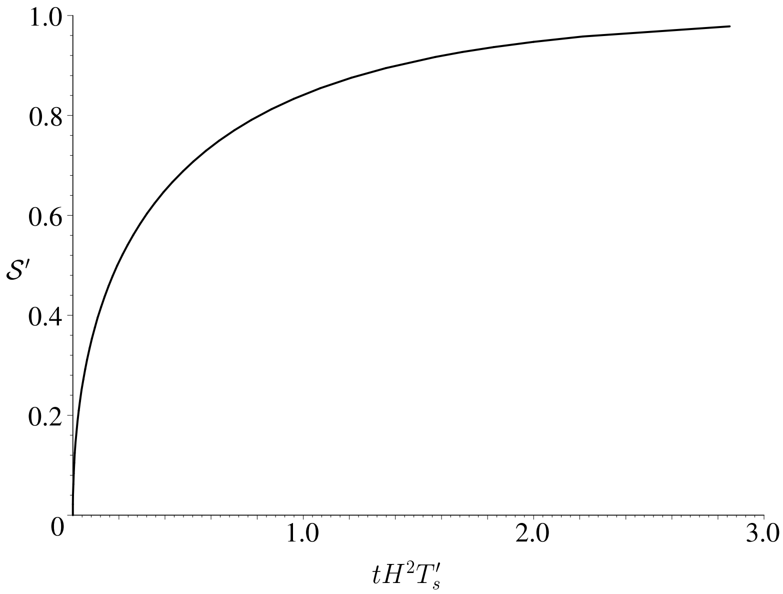

Figure 12: A plot of the solution to equation (23), as $\mathcal{S}'$ versus tH^2T_s'.

As noted above, early time behaviour is the same as for zero heat transfer,

$$\mathcal{S} \sim \sqrt{2\,t\,/T_s'}\ , \tag{24}$$

and this behaviour is only valid for times

$$t \ll \frac{1}{2H^2T_s'}\ . \tag{25}$$

Using $T_s' \approx 0.22$, an estimate of early time (in seconds) is

$$\tilde{t} \ll \frac{10^{-5}}{4\kappa_{\text{ bed}}}\ ,$$

so that for $\kappa_{\text{ bed}}$ in the range 10^{-7} to 10^{-9} m^2/s, early time is

$$\tilde{t} \ll 25 - 2500 \text{ s}\ .$$

This suggests that if coatings are dipped for only 5–10 seconds, the early time approximation is likely to be a good one.

7 Estimates of Coating Thickness Based on Models

All models predict a coating thickness that grows initially as the square root of time. The coating grows faster if the temperature difference between the iron casting and the fluidised bed is increased.

The simple conduction model for upwards-facing surfaces depends on the parameter β, which is given by

$$T_s = \mathrm{erfc}(\beta) \ ,$$

and upon the nondimensionalisation of time, $\tilde{t} = t/\kappa_{\text{ bed}}$, where $\tilde{t}$ is in seconds.

Using $T_s = 0.18$, which corresponds to an initial casting temperature of 200°C, a bed temperature of 30°C, and a sticking temperature of 60°C, gives $\beta = 0.95$. Then using $\kappa_{\text{ bed}} = 6 \times 10^{-7}$ m^2/s, the coating thickness is, according to the simple conduction model,

$$s = 2\beta\sqrt{t} \approx 0.0015\sqrt{\tilde{t}} \ . \tag{26}$$

The melted-on model for downwards-facing surfaces depends on the parameter α, which is given for early times by

$$T_s = 1 - \sqrt{\pi}T_s\alpha e^{\alpha^2}\mathrm{erf}(\alpha) \ .$$

If $T_s = 0.18$, this gives $\alpha = 1.03$. In fact, β is less than α in general, as illustrated in Figure 13, which is a plot of values of α (solid line) and β (dashed line) for various values of T_s, obtained using Maple.

Then the melted-on model predicts the coating thickness on downwards-facing surfaces for early times to be

$$\mathcal{S} = 2\alpha\sqrt{t} = 2\alpha\sqrt{\kappa_e}\sqrt{\tilde{t}} \ . \tag{27}$$

Using $\kappa_e \approx 10^{-7}$ m^2/s and $\alpha \approx 1.03$ gives

$$\mathcal{S} \approx 0.00068\sqrt{\tilde{t}} \ . \tag{28}$$

This is a little less than one-half of the thickness predicted in equation (26) for upwards-facing surfaces, and is in surprisingly good agreement with our measurements of coating thickness, considering the uncertainty in thermal properties of bed and melted epoxy.

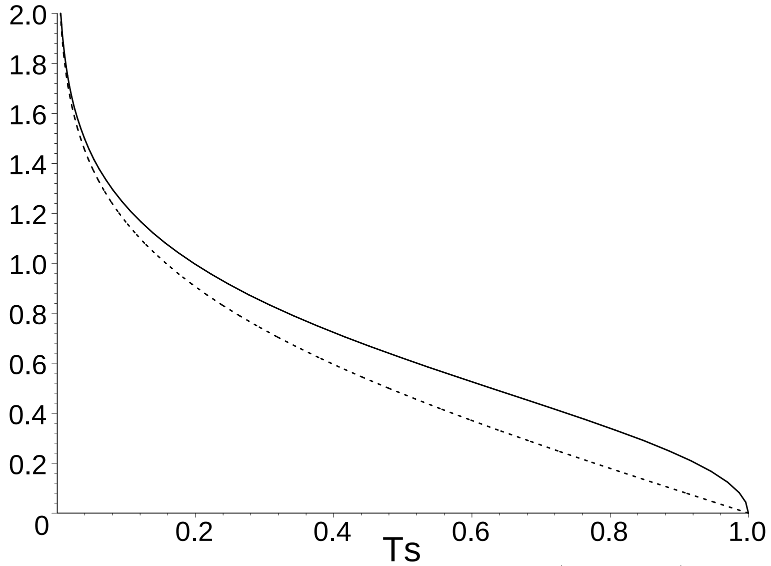

Figure 13: A plot of values of the parameters α (solid line) and β (dashed line) against values of T_s.

It is also of interest to note the predicted coating thickness from the early time linear temperature approximation,

$$\mathcal{S} = \sqrt{\frac{2t}{T_s'}} = \sqrt{\frac{2\kappa_e \tilde{t}}{T_s'}} \approx 0.001\sqrt{\tilde{t}}\,. \tag{29}$$

This is about half as large again as the melted-on model prediction, but still in reasonable agreement with it. We would expect that the linear temperature model would over-estimate coating thickness, as the actual temperature gradient driving the coating surface into the bed will be less that the linear one used here.

That is, at early times the downward-facing surfaces grow at about half the rate of upward-facing surfaces. At later times this difference will be exacerbated by the fact that the growth-rate of the downward-facing surfaces will slow down as the horizontal asymptote is approached.

8 Obtaining a More Even Coating

Since downward facing surfaces have a coating that is thinner than upwards-facing surfaces, one way to obtain a more even coating is to swap them over during the immersion process. At first glance it seems reasonable to swap them halfway through, but this assumes that the coating grows linearly in time. The early time behaviours give coating thicknesses that grow as the square root of time. Then the correct time to swap upper and lower surfaces is after one-quarter of the total dipping time ($\tilde{t}_f$ seconds) has elapsed, and the total coating thickness after $\tilde{t}_f$ seconds is then given by

$$\langle S \rangle = (\alpha\sqrt{\kappa_e} + \beta\sqrt{\kappa_{\text{bed}}})\sqrt{\tilde{t}_f} \ . \tag{30}$$

For the values used above, this becomes

$$\langle S \rangle \approx 0.0011\sqrt{\tilde{t}_f} \ , \tag{31}$$

where $\langle S \rangle$ is in metres and $\tilde{t}_f$ is in seconds.

However, the estimated time for the coating thickness to reach 400 μm is then $\tilde{t}_f \approx 0.13$ s, which is a factor of 20 too small according to experiments conducted by Toowoomba personnel. This reflects our uncertainty in the effective thermal properties of fluidised bed and melted epoxy. The qualitative behaviour of coating thickness should be useful though, especially the dependence on the square root of time, and the rather complicated dependence on temperatures.

9 Order of magnitudes

symbol	value	units	comments
	1–2	s	cross film heat diffusion time
	0.05	s	cross epoxy particle diffusion time
	1.5–3	°K	exothermic setting causes ΔT in casting
U_{mf}	0.003	m/s	fluidisation velocity for epoxy
	10	°C	temperature drop of casting if immersed for 5s
σ_e	0.001	kg/s^2	surface tension of epoxy

Experiments were carried out placing a teaspoon of epoxy powder in a heap on hot castings (various temperatures were used). Each heap was about 50 mm long, 20 mm wide and roughly 7–9 mm high in a pyramidal type shape. The time in seconds from placement to when the surface set was measured as shown in the following table.

180 °C	190 °C	200 °C	210 °C	220 °C
45	32	35	40	25
25	31	35	35	20

The final film thickness may have been perhaps 2 mm at its thickest. The melt did seem to flow a little but we are not at all sure how much. The epoxy did not seem to wet the casting.

10 Thin film flow

The film of epoxy particles does seem to flow to some extent before it gelatinises because it is reported that the casting is pulled out of the bed with a "furry" surface that then smooths. However, we have no reasonable idea of the epoxy melt viscosity or surface tension coefficient.

The gel time is almost certainly temperature dependent as the data for the similar product Scotchkote shows, see Table 1. Assuming the same slope for NAP-GARD leads to the law

$$t_{\text{gel}} = 15\, e^{-0.0141\,(T-200)}\,\mathrm{s}\,, \tag{32}$$

as tabled below (to errors of at least 20%)

temperature (°C)	gel time (s)
160	26
180	20
200	15
220	11
240	8.5

Note that the gelatinising process of the epoxy is exothermic. We estimate that this should heat up the casting by 1.3 °C over the gel time. Since most of this will be after the casting has been pulled out of the fluidised bed, and casting temperatures may drop by about 10°C in the bed, and temperatures are planned to be high enough above the melting temperature of 70°C that coating rates are not very sensitive to actual temperature, we consider that this will not significantly affect the thickness of the epoxy coating.

Before it gels, the flow of the thin film on the complex curvature of the casting may evolve according to [15], so that

$$\frac{\partial\zeta}{\partial t} \approx -\frac{\sigma_e}{3\mu_e}\boldsymbol{\nabla}\cdot\left[\eta^2\zeta\boldsymbol{\nabla}\tilde{\kappa} - \frac{1}{2}\eta^4(\kappa\mathbf{I}-\mathbf{K})\cdot\boldsymbol{\nabla}\kappa\right], \tag{33}$$

where $\zeta = \eta - \frac{1}{2}\kappa\eta^2 + \frac{1}{3}k_1k_2\eta^3$ is proportional to the amount of fluid locally above the substrate; $\mathbf{K}$ is the curvature tensor of the substrate; k_1, k_2, and $\kappa = (k_1 + k_2)/2$ are the principal curvatures and the mean curvature of the substrate, respectively; and the ∇-operator is expressed in a coordinate system of the substrate. This assumes the Reynolds number is small enough[1] and that there are no significant property variations across the thin film melt and none in time. But in the absence of any estimates of the surface tension coefficient, σ_e, nothing quantitative can be done with this model.

11 Recommendations

- Use a hot oven (about 300°C) to heat castings to near 200°C in a reasonable time (about 20 minutes).
- Turn the casting upside down while in the fluidised bed a quarter of the time into the coating process, in such a way as to swap downward-facing surfaces and upward-facing surfaces, to help make the coating more even.
- Dip the casting in a way that ensures that the first part to enter the bed is the first part to leave the bed. This will equalise the time spent in the bed by different parts of the casting—this is especially important for big castings.
- Coating thickness should grow as the square root of time, so dip for four times as long to get twice the thickness.
- Raising the temperature of the fluidised bed, while still keeping it below T_s, will speed up coating growth.
- Raising the initial casting temperature will speed up coating growth.

Acknowledgements

Many contributors gave of their time and expertise to this problem, including in alphabetical order Noel Barton, Grant Cox, Neville Fowkes, John Hewitt, Ian Howells, Phil Howlett, John King, Sean McElwain, Robert McLachlan, Colin Please, and Kiren Williams.

We also thank the personnel from Toowoomba Foundry for their great support and time and first-hand knowledge of the problem, especially Mithiran Kirupairajah, Alex Wright and Gary Schultz.

[1] If the Reynolds number is not so small, then a more refined model is given by Li & Roberts [12].

And a special thank-you to Sean McElwain, the Director of the Study Group, for the excellent technical support, books and reprints that were so essential to the progress we made.

References

[1] Standards Australia and Standards New Zealand, Australian/New Zealand Standard: thermal-bonded polymeric coatings on valves and fittings for water industry purposes, Technical report, Standards Australia and Standards New Zealand, 1996.

[2] J.F. Davidson and D. Harrison, editors, *Fluidization*, Academic Press, 1971.

[3] J.F. Davidson and D. Harrison, *Fluidised Particles*, Cambridge University Press, 1963.

[4] Dulux. NAP-GARD 7-2501 thermosetting epoxy powder pipe coating, Technical report, Dulux, June 1989.

[5] M. Elmas. *Fluidised bed powder coating*, volume **5** of *Powder Tech Pub Series* Powder Advisory Centre.

[6] N.I. Gelperin and V.G. Einstein, Heat transfer in fluidized beds, In J.F. Davidson and D. Harrison, editors, *Fluidization*, chapter 10, pages 471–540. Academic Press, 1971.

[7] C. Gutfinger and W.H. Chen, Heat transfer with a moving boundary — application to fluidised-bed coating, *Int. J. Heat Mass Transfer,* **12**, pages 1097–1108 (1969).

[8] D. Harrison and J.R. Grace, Fluidized beds with internal baffles, In J.F. Davidson and D. Harrison, editors, *Fluidization*, chapter 13, pages 599–626. Academic Press, 1971.

[9] B. Hirschberg and J. Werther, Factors affecting solids segregation in circulating fluidized-bed riser, *AIChE Journal*, **44**, pages 25–34, 1998.

[10] J.P.Holman, *Heat Transfer,* McGraw-Hill, 1990.

[11] K.C. Leong, G.Q. Lu, S.K. Bhatia and V. Randolph, Modelling of heat transfer in fluidised-bed coating of thin plates, *Chemical Engineering Science,* **53**(6), pages 1307–1310 (1998).

[12] Zhenquan Li and A.J. Roberts. The accurate and comprehensive model of thin fluid flows with inertia on curved substrates. Technical report,

[http://xxx.lanl.gov/abs/chao-dyn/9906011], June 1999. submitted to IMA J Appl Math.

[13] J.F. Richardson, Incipient fluidization and particulate systems, In J.F. Davidson and D. Harrison, editors, *Fluidization*, chapter 2, pages 26–64. Academic Press, 1971.

[14] W.M. Rohsenow, J.P. Hartnett and E.N. Ganic, *Handbook of heat transfer fundamentals,* McGraw-Hill, 1985.

[15] R. Valery Roy, A.J. Roberts, and M.E. Simpson, A lubrication model of coating flows over a curved substrate in space. Technical report, [http://xxx.lanl.gov/abs/patt-sol/9705002], August 1997.